

Analysis of Ionospheric Scintillation and Its Impact on PPP at Low Latitudes

Kai Guo, Marcio Aquino, Sreeja Vadakke Veetil, *University of Nottingham*
Zhizhao Liu, Wu Chen, *the Hong Kong Polytechnic University*
Haroldo Antonio Marques, *Military Institute of Engineering (IME)*

BIOGRAPHIES

K. Guo is a Marie Skłodowska-Curie research fellow at the Nottingham Geospatial Institute of the University of Nottingham in the UK, within the TREASURE project funded by the European Union's Horizon 2020 Research and Innovation Programme. He concentrates on developing novel GNSS receiver tracking models and scintillation mitigation tools, aiming to improve the receiver tracking performance under ionospheric scintillation.

M. Aquino is an Associate Professor at the Nottingham Geospatial Institute of the University of Nottingham in the UK. He pioneered the deployment of ionospheric scintillation and TEC monitoring receivers in Northern Europe in 2001. His research has focused on ionospheric effects on GNSS, including system vulnerability to ionospheric disturbances and relevant countermeasures.

S. Vadakke Veetil is a senior research fellow at the Nottingham Geospatial Institute of the University of Nottingham in the UK, involved in European Commission, European Space Agency and UK research council funded projects. Her research focuses on assessing the effects of space weather on GNSS receivers and positioning errors aiming to improve the modeling of scintillation and to develop scintillation mitigation tools.

Z. (George) Liu currently is an Associate Professor at the Department of Land Surveying and Geo-Informatics (LSGI), The Hong Kong Polytechnic University (PolyU), Hong Kong, P. R. China. He received his BSc degree in Surveying Engineering from the Jiangxi University of Science and Technology, China, in 1994 and MSc degree in Geodesy from the Wuhan University, China, in 1997. He earned his PhD in Geomatics Engineering from the University of Calgary, Canada, in 2004. His research interests include GNSS algorithm development for precise positioning and navigation, atmospheric water vapor observation and ionosphere TEC and scintillation monitoring.

W. Chen is Professor at Department of Land Surveying and Geo-Informatics, Hong Kong Polytechnic University. Prof Chen has been actively working on GNSS related research for more than 30 years. His main research interests are GNSS positioning technologies, system integrity, various GNSS applications, seamless positioning, and SLAM.

H. Antonio Marques received his BSc degree in Cartographic Engineering in 2005, MSc in Cartographic Science in 2008, and PhD in Cartographic Science in 2012 at Sao Paulo State University (UNESP), Presidente Prudente in Brazil. From 2011 until 2016, he worked as Adjunct Professor at the Department of Cartographic Engineering, Federal University of Pernambuco (UFPE), Recife in Brazil. Since then, he has been teaching at Military Institute of Engineering (IME), Rio de Janeiro in Brazil, where he is lecturing and researching topics related to Geodesy and Adjustment, especially those related to GNSS, surveying, and atmospheric sciences.

ABSTRACT

Ionospheric scintillation refers to the random and rapid fluctuations in the amplitude and phase of radio signals that occur due to their propagation through plasma density irregularities in the ionosphere. For Global Navigation Satellite System (GNSS), scintillation can seriously degrade satellite signal quality and consequently the positioning accuracy, particularly at high and low latitude regions, where ionospheric disturbances are more frequent. This study analyzes the effects of scintillation on Global Positioning System (GPS) Precise Point Positioning (PPP), by making use of scintillation data recorded in Hong Kong during the solar maximum of 2014. Significant positioning error values of as much as 1.34 m in the up direction are observed with kinematic PPP processing under strong scintillation. The variations in the standard deviations of the carrier phase residuals in relation to satellite elevations and scintillation levels are investigated for the first time in this region. It is found that the standard deviation of carrier phase residuals increases depending on scintillation intensity. This study is important to help better understand the scintillation characteristics and its effects on GPS-based positioning in the Hong Kong region. It can also help in modelling the relationship between scintillation and carrier phase residuals, which can be of use in the development of scintillation mitigation approaches for PPP processing.

Keywords: Ionospheric scintillation, GPS, kinematic PPP, carrier phase residuals

INTRODUCTION

Ionospheric scintillation refers to the rapid fluctuations in amplitude and phase of a radio signal when it propagates through the plasma density irregularities in the ionosphere [1]. Basu et al. [2] pointed out that the occurrence of scintillation is related to solar and geomagnetic activities. In the solar maximum years, the probability of scintillation occurrence can be enhanced, especially at equatorial, auroral and polar latitudes. The occurrence of ionospheric scintillation presents large day-to-day variability and it mainly concentrates on the period between post-sunset and midnight hours at low latitudes. To Global Navigation Satellite System (GNSS) users, scintillation is a crucial and challenging interference, posing serious threats to safety-critical applications and precise positioning.

In the presence of ionospheric scintillation, the quality of GNSS signals can be adversely affected, leading to the degradation in the GNSS receiver tracking loop performance and consequently of positioning accuracy [3-6]. As the signal amplitude rapidly fluctuates due to scintillation, the code phase alignment becomes inaccurate and acquisition becomes more difficult for the receiver Delay Locked Loop (DLL), leading to degraded code measurements. On the other hand, the rapid phase fluctuations lead to decreased accuracy of phase estimation in the receiver Phase Locked Loop (PLL), which results in degraded phase measurements. In severe scintillation conditions, the receiver could even suffer from cycle slips or/and complete loss of lock. These degraded code and phase measurements contribute to larger positioning errors.

The effects of scintillation on GNSS positioning has drawn extensive attention in recent years. [7] studied the ionospheric scintillation characteristics across the Global Positioning System (GPS) frequency band using scintillation data collected at the Arctic auroral zone. It was concluded that the increase in carrier phase measurement noise due to scintillation could bring significant errors to Precise Point Positioning (PPP). Linty et al. [8] investigated the high-latitude phase scintillation effects on GPS positioning during the geomagnetic storm of September 2017. The results showed that moderate and strong phase scintillation could severely affect the carrier smoothing algorithms and the positioning errors calculation doubled in magnitude under scintillation. Park et al. [9] pointed out that the performance of kinematic positioning is generally poor under strong scintillation conditions at low latitudes in Brazil. It was demonstrated that by estimating the tracking errors caused by scintillation and using them to modify the stochastic model in the least squares adjustment used for position calculation, the positioning accuracy could be improved. The effects of low-latitude scintillation on the BeiDou Navigation Satellite System (BDS) were investigated by [10]. It was found that the code and phase residuals of static PPP processing could reach up to 7.096 and -0.469 m, respectively. Significant errors in the east, north and up directions could be observed in kinematic PPP calculation. However, these analyses mainly concentrate on investigating the adverse effects of scintillation on positioning. The relationship between scintillation levels and the measurement errors are not considered explicitly.

This study focuses on the effects of ionospheric scintillation on PPP in Hong Kong, which is in a low-latitude region and where the scintillation occurrence is frequent. The correlation between the variation of carrier phase residuals and scintillation levels as well as the satellite elevations is analyzed for the first time. In the following section, scintillation indices and PPP processing set up are introduced first. The data set and the Ionospheric Scintillation Monitoring Receiver (ISMR) are then described. Results are shown and discussed next, followed by the conclusions and remarks.

SCINTILLATION INDEX

Ionospheric scintillation is categorized as amplitude and phase scintillation, commonly characterized by the widely used indices $S4$ and σ_ϕ , respectively. $S4$ is defined as the standard deviation of the detrended signal power normalized by its average [11, 12]:

$$S4 = \sqrt{\frac{\langle P_{det}^2 \rangle - \langle P_{det} \rangle^2}{\langle P_{det} \rangle^2}} \quad (1)$$

where P_{det} is the detrended signal power measurements and $\langle \cdot \rangle$ denotes the arithmetic mean calculation. $S4$ is usually computed every 60 s and it directly describes the strength of signal power fluctuation. Similarly, σ_ϕ is defined as the standard deviation of the detrended carrier phase within 60 s [13]:

$$\sigma_\phi = \sqrt{\langle \phi_{det}^2 \rangle - \langle \phi_{det} \rangle^2} \quad (2)$$

where ϕ_{det} is the detrended carrier phase measurements. Other indices commonly used to determine the intensity of phase scintillation are the power spectral parameters, in particular the spectral slope (p) and the spectral strength at 1 Hz (T) calculated by

the spectral analysis of the detrended carrier phase measurements. For more details on the power spectral parameters for scintillation analysis readers are referred to [14].

Figure 1 shows an example of strong fluctuations in signal power and carrier phase measurements due to ionospheric scintillation captured on GPS L1CA signal of GPS SV 22 between 20:00 to 21:30 Local time (LT) on 10 November 2014 in Hong Kong. It can be seen from the top two panels that strong scintillation occurs at around 20:30 LT, when the satellite elevation is around 55°. The scintillation lasts about 40 minutes and then disappears at around 21:10 LT. Meanwhile, from the two panels at the bottom, it is obvious that both the signal power and the carrier phase measurements suffer apparent fluctuations which are approximately modulated by the intensity of scintillation. Analyzing all 4 panels of Figure 1, it becomes clear that when there is no scintillation the signal power and carrier phase measurements only present slight variations, which are due to the ambient noise.

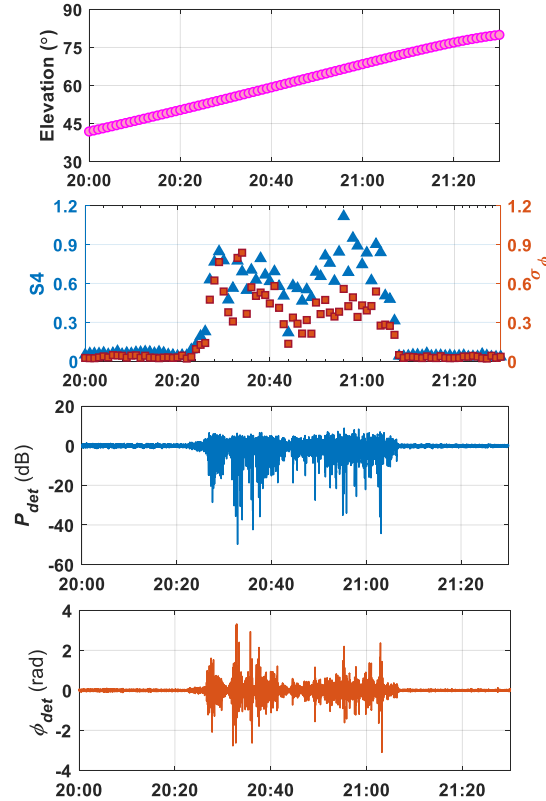


Figure 1. Adverse effects of ionospheric scintillation on GPS L1 C/A signal power and carrier phase measurements for SVID 22 observed from 20:00 to 21:30 (LT) on 10 November 2014 in Hong Kong. The plots respectively show the variations of satellite elevation and scintillation index (the top two panels) and the detrended signal power and carrier phase measurements (the bottom two panels)

For more details on the high-frequency intensity and carrier phase measurement detrending process, readers may refer to [12]. Both S_4 and σ_ϕ analyzed in this study are calculated using the high frequency measurements output from the ISMR deployed at the station in Hong Kong. The details of the data set and the receiver will be explained next.

PPP MODELS AND ALGORITHMS

The PPP processing is accomplished by the RT_PPP software [15]. GPS code and carrier phase observations on both the L1 and L2 frequencies are processed at a sampling rate of 1 s. A satellite elevation mask angle of 15° is set. The ionospheric-free linear combination is applied to mitigate the first-order effects of the ionosphere. International GNSS Service (IGS) precise clock and orbit products are used. The models and PPP calculation strategies are summarized in Table 1. With these settings, the non-scintillation effects on PPP calculation can be minimized.

Table 1. Models and algorithms applied in the PPP processing

Items	Algorithms
Observations	GPS code and carrier phase observations on L1 and L2 signal (L1CA, ϕ_1 , L2P, ϕ_2)
Observation weighting	The inverse sine of satellite elevations
Sampling interval	1 s
Elevation mask angle	15°
Ionospheric delay	Ionospheric-free linear combination
Satellite orbit	IGS orbits correction
Satellite clock	IGS clock correction
Tropospheric delay	Troposphere estimated as a random walk process ($0.05\text{m}/\sqrt{\text{hour}}$)
Receiver coordinate	Static and kinematic models
Others	Absolute phase center variation (PCV) correction, ocean tide loading (OTL) correction, Differential Code Biases (DCB) correction

DATA SET

The scintillation data analyzed in this study were collected at Hok Tsui (Lat. 22 ° 12 'N, Long. 114 ° 15 'E, Magnetic Lat. 12.67 °N) in Hong Kong, denoted as HKHT station. This station is equipped with a Septentrio PolaRxS Pro receiver, which is capable of tracking GPS, GLONASS, Galileo and BDS signals and is dedicated for ionospheric monitoring. The receiver can generate 50 Hz or 100 Hz amplitude and carrier phase measurements, as well as amplitude and phase scintillation indices at a rate of 1 min. It should be noted that the Septentrio receiver can capture and output scintillation index on L1CA and L2C signals. According to [3, 16], the S_4 and σ_ϕ on L2P can be calculated as:

$$S_4(\text{L2P}) = \left(\frac{f_1}{f_2}\right)^{1.5} * S_4(\text{L1CA}) \quad (3)$$

$$\sigma_\phi(\text{L2}) = \left(\frac{f_1}{f_2}\right) * \sigma_\phi(\text{L1}) \quad (4)$$

where f_1 and f_2 are the L1 and L2 frequencies, respectively. Therefore, the scintillation on L2P is proportional to and larger than that on L1CA theoretically.

Based on scintillation activity, scintillation data and nominal carrier and code data recorded on GPS L1 and L2 signals on November 10, 2014 are chosen for the analysis. For comparison, data recorded on November 9, 2014, when scintillation is weaker, are also analyzed.

SCINTILLATION OCCURRENCE

In this section, scintillation data recorded on GPS L1 signals at HKHT on November 9 and 10 is studied first to give an overall view of the scintillation occurrences in Hong Kong. Figure 2 shows the occurrence of scintillation observed from all the visible satellites on these two days. As it can be seen from the top panel, there is only few scintillation occurrence on 9 November. However, it can be seen in the bottom panel that both amplitude and phase scintillation occur frequently. On 10 November, the number of amplitude scintillation events with $S_4 > 0.3$ and phase scintillation events with $\sigma_\phi > 0.3$ are 298 and 186, respectively. It can also be noticed that almost all the scintillation events occur at post-sunset time, from around 20:00 LT to midnight, which agrees with the previous conclusions by [17].

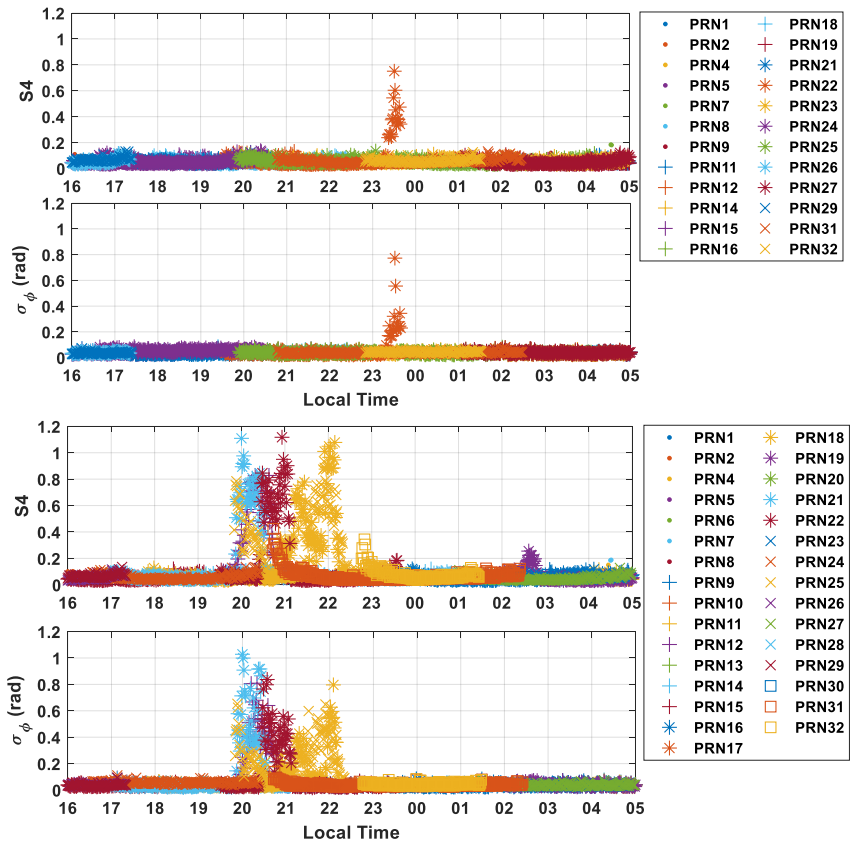


Figure 2. Occurrence of amplitude and phase scintillation observed from all the visible satellites on 9 (top) and 10 (bottom) November 2014

The distributions of amplitude and phase scintillation in relation to intensity levels are further shown in Figure 3. As scintillation occurrence on 9 November is mostly negligible, only the results for 10 November are presented. From the figure, it can be observed that the occurrence of phase scintillation is mostly characterized by values of σ_ϕ less than 0.6, with very few occurrences when σ_ϕ is over 0.7. By contrast, the occurrence of amplitude scintillation is mostly characterized by values of $S4$ between 0.3 and 0.8 on this day, confirming that amplitude scintillation is more frequently observed than phase scintillation at these latitudes [17]. It should be noted that in order to minimize multipath interference on the analysis, only receiver/satellite links over 30° elevation angle are considered in Figures 2 and 3.

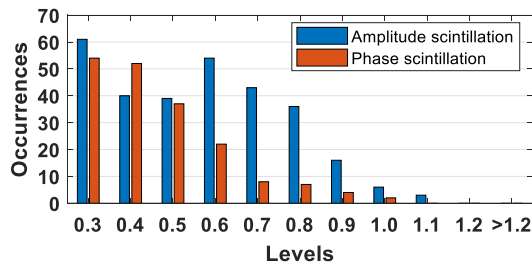


Figure 3. Distributions of amplitude and phase scintillation in relation to scintillation levels on 10 November 2014

SCINTILLATION EFFECTS ON PPP

The adverse effect of ionospheric scintillation on PPP processing is demonstrated in this section. In PPP, both the number and the geometry distribution of the visible satellites can affect the positioning accuracy. Figure 4 shows the number of visible and scintillation affected satellites on 9 and 10 November 2014. A lower threshold of 0.2 for both amplitude and phase scintillation is adopted to determine whether the signals are affected. It can be seen that the time series of the total number of visible satellites follows a similar patterns on these two days. In terms of satellites affected by scintillation, only a few satellites are observed to meet this criterion on 9 November. However, on 10 November, the number of satellites simultaneously affected by amplitude or phase scintillation increases dramatically at around 20:00 LT. For the amplitude scintillation affected satellites, the number can even reach up to 5 at times.

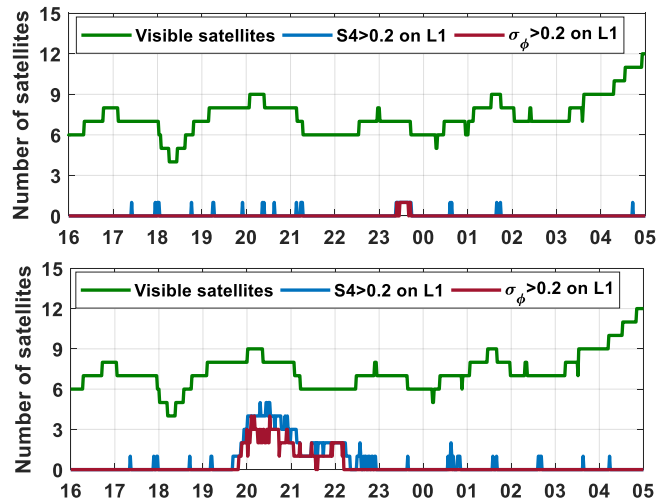


Figure 4. Numbers of visible and scintillation affected satellites in relation to local time on 9 (top) and 10 (bottom) November 2014

Static and kinematic PPP solutions are then processed and the results are analyzed on both 9 and 10 November. The final coordinates calculated by static PPP on 9 November are set as the reference coordinates. The PPP positioning errors measured in east (ΔE), north (ΔN), and up (ΔU) directions are shown in Figure 5. As it can be seen from the left-top and right-top panels, the positioning errors of static PPP calculation on both days are relatively stable, within -0.05 m and $+0.05$ m after convergence. However, the kinematic PPP positioning errors present obvious fluctuations on both days. Compared with 9 November, the kinematic positioning errors present significantly higher values, particularly from around 20:00 to 23:00 LT. This difference mainly results from scintillation effects, as the observational satellite geometric configurations are similar on both days. It is worth mentioning that the gaps in both panels, seen between 18:10 and 19:00 LT, are not caused by scintillation, as it can be observed from Figure 4 that the total number of visible satellites decreases to 4 at around 18:20 on both days, which probably leads to the failures in PPP processing.

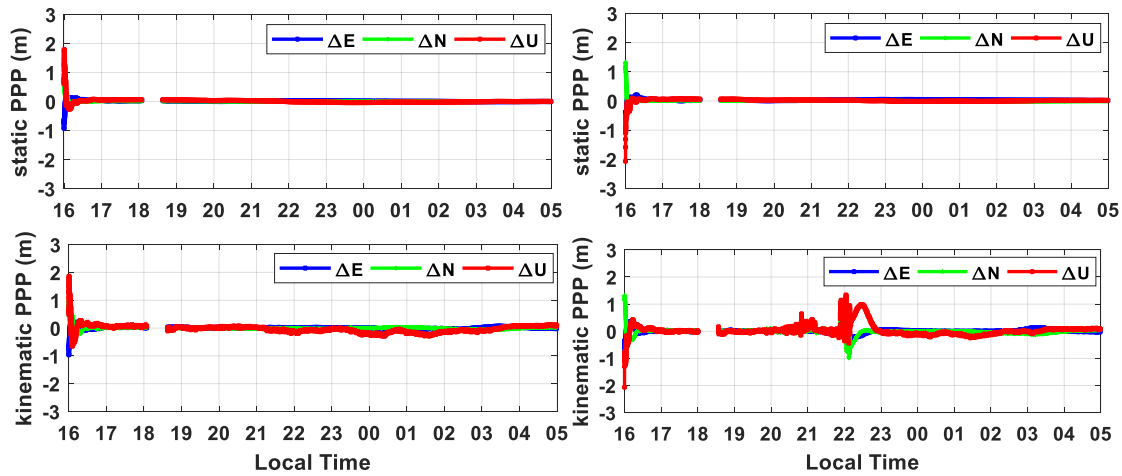


Figure 5. Static and kinematic PPP positioning errors measured in east, north, and up directions on 9 (left) and 10 (right) November 2014

The root mean squares (RMS) and maximum of the ΔE , ΔN and ΔU on November 9 and 10 are summarized in Table 2. It should be noted that the first 4 hours are not considered in the calculation due to the convergence time and processing gaps. As shown in the table, the RMS and maximum errors for kinematic PPP calculation are larger than the static PPP calculation on both days. Additionally, by comparing the kinematic PPP positioning errors between these two days, the RMS and maximum of positioning errors in the east, north and up directions on 10 November are much larger than on 9 November. The RMS error in the north direction is 0.234 m, which is almost 4 times as much as that on 9 November. Moreover, compared with the positioning results in the east and north directions, the results in the up direction are seen to be more affected by scintillation for all the situations.

Table 2. RMS and the maximum of ΔE , ΔN and ΔU on 9 and 10 November 2014 (in meters)

Date	PPP Models	RMS ΔE	RMS ΔN	RMS ΔU	Max ΔE	Max ΔN	Max ΔU
09/11/14	Static	0.0111	0.0052	0.0232	0.0232	0.0109	0.0389
	Kinematic	0.0254	0.0295	0.1203	0.0786	-0.1113	-0.3079
10/11/14	Static	0.0340	0.0093	0.0189	0.0514	0.0128	0.0362
	Kinematic	0.0621	0.1158	0.2340	-0.3161	-0.9864	1.3369

CARRIER PHASE RESIDUAL ANALYSIS UNDER SCINTILLATION

Satellite positioning calculation is based on measuring the ranges between the receiver and visible satellites. In the presence of scintillation, the accuracy of the range measurements can be affected to varying degrees. Therefore, it is interesting to know the relationship between the scintillation levels and the range measurement errors. In this section, correlation analyses are carried out to statistically characterize amplitude and phase scintillation effects on the carrier phase residuals. As the scintillation occurrences on 9 November are few, only the data on 10 November is considered for the study.

Figure 6 shows the time series of satellite elevations and static PPP carrier phase residuals on 10 November. In the bottom panel, the carrier phase residuals of all the satellites are small, between -0.05 m to +0.05 m, when the scintillation occurrence is low between 00:00 to 05:00 LT which can be seen in the bottom panel of Figure 2. However, for SVID 18, SVID 21, SVID 22 and SVID 25, the phase residuals suffer from obvious fluctuations from around 19:40 to 23:00 LT, which is exactly the period when frequent amplitude and phase scintillation occur, as indicated in Figure 2 and Figure 4.

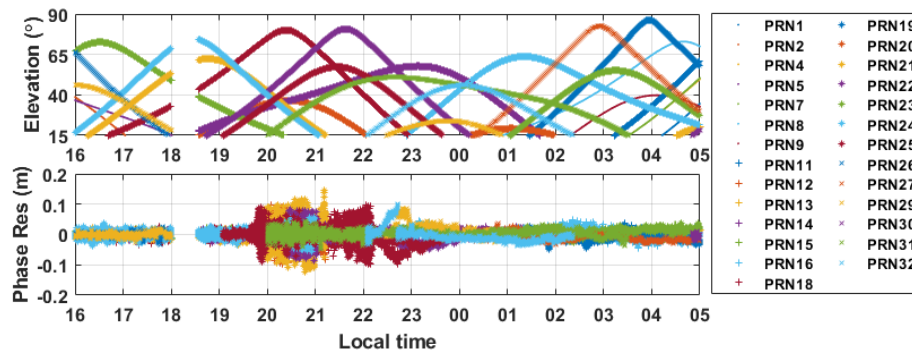


Figure 6. Satellite elevations (top) and static PPP carrier phase residuals (bottom) in relation to local time on 10 November 2014

To further investigate the effects of scintillation on carrier phase residuals, the standard deviations of static PPP carrier phase residuals at every 60 s are calculated. Figure 7 presents the satellite elevation, amplitude and phase scintillation levels along with the standard deviations of ionosphere-free carrier phase residuals for SVID 25 on 10 November. As can be seen from the top and middle panels, amplitude and phase scintillation occur at around 19:40 and 21:30 LT, when the satellite elevations are around 30 ° and 50 °, respectively. At the same time, the standard deviations of carrier phase residuals in the bottom panel increase roughly in agreement with the scintillation intensity approximately, which means the measurement errors are strongly correlated to the amplitude and phase scintillation levels.

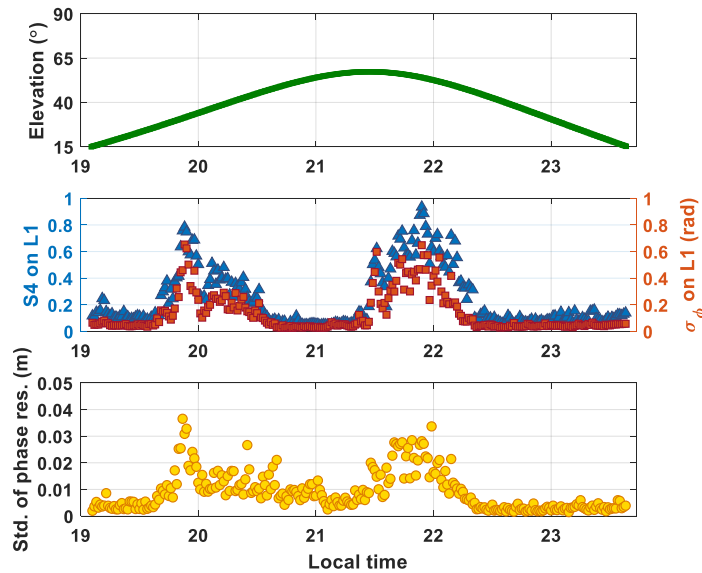


Figure 7. Time series of satellite elevations, amplitude and phase scintillation levels and the standard deviation of carrier phase residuals for SVID 25 on 10 November 2014

Figure 8 shows the correlation analysis between the standard deviations of carrier phase residuals and the amplitude and phase scintillation levels for SVID 25 on 10 November. It can be seen from the panels that the scintillation levels are highly correlated with the standard deviation of carrier phase residuals. The correlation coefficients can reach up to 0.8262 and 0.8442 for S_4 and σ_ϕ , respectively.

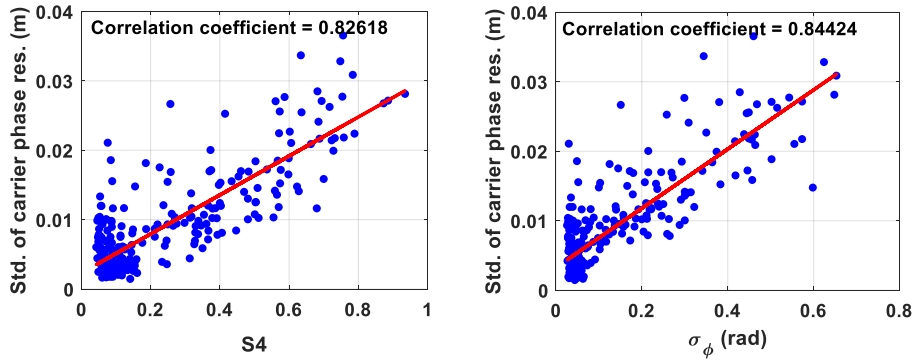


Figure 8. Correlation analysis between the standard deviation of carrier phase residuals and the $S4$ (left) and σ_ϕ (right) for SVID 25 on 10 November 2014

The variation of the standard deviation of phase residuals in relation to elevation angle and scintillation levels is then analyzed and the results are shown in Figure 9. The different levels of scintillation are grouped according to: Non-scintillation for $S4$ or $\sigma_\phi < 0.1$; Weak for $S4$ or σ_ϕ between 0.1 and 0.3; Moderate for $S4$ or σ_ϕ between 0.3 and 0.5; Strong for $S4$ or σ_ϕ between 0.5 and 0.7 and extremely strong for $S4$ or $\sigma_\phi \geq 0.7$. Then the standard deviations of carrier phase residuals for the various scintillation levels are averaged according to the satellite elevation angles. It can be seen from the figure that the standard deviation of phase residuals varies slightly with the increase in satellite elevation under the same amplitude or phase scintillation levels. However, the standard deviations increase gradually when the scintillation levels increase, for the same satellite elevation. When there is no scintillation, the standard deviations of phase residuals are lower than 0.005 m for all elevations. Nonetheless, residuals could reach 0.015 m for moderate scintillation, 0.02 m for strong scintillation and 0.03 m for extremely strong scintillation, which means both the amplitude and phase scintillation can greatly affect the carrier phase measurement errors.

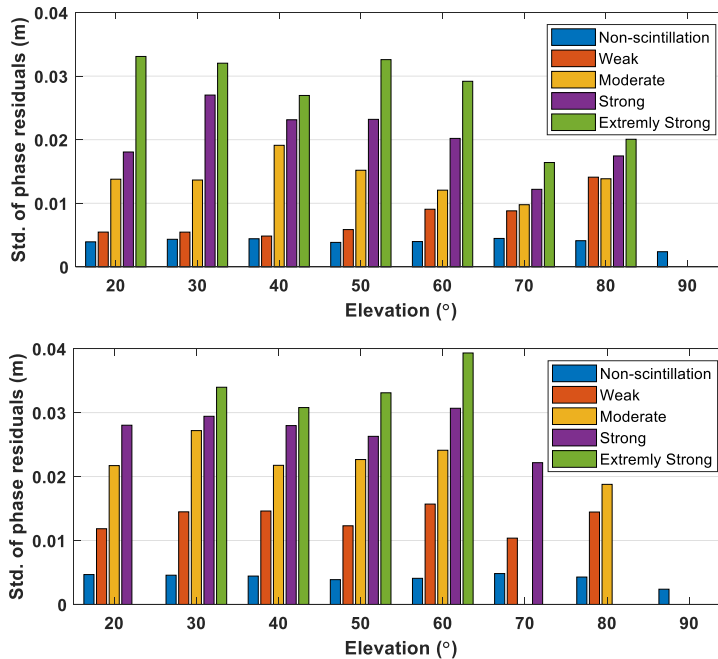


Figure 9. Variation of the standard deviation of carrier phase residuals in relation to elevations and amplitude (top) and phase (bottom) scintillation levels

CONCLUSION AND REMARKS

This study analyzed ionospheric scintillation data captured in Hong Kong during the solar maximum of 2014. The adverse effects of scintillation on PPP were investigated. Relationships between the fluctuations of carrier phase residuals, scintillation levels and satellite elevation were further studied. Based on these analyses, the following conclusions can be drawn:

1. A strong and frequent occurrence of ionospheric scintillation was observed in the Hong Kong region. On November 10, scintillation mostly occurred between post-sunset time and midnight local time, and the number of satellites simultaneously affected by scintillation could reach up to 5. Additionally, the distribution of scintillation occurrence for each of the two scintillation indices indicated that amplitude scintillation was more frequent than phase scintillation on 10 November 2014.
2. Analysis of scintillation effects on PPP showed that amplitude scintillation at low latitudes could greatly influence the positioning accuracy of kinematic PPP. The positioning errors in the east, north and up directions exhibited significant fluctuations in the presence of scintillation on November 10. Compared with the positioning results in the east and north directions, the positioning result in the up direction was seen to be more affected by scintillation. The maximum positioning error in the up direction was 1.3369 m on November 10, whereas on November 9, with low scintillation occurrence, it was only -0.3079 m.
3. Fluctuations of carrier phase residuals were observed to be strongly correlated to amplitude and phase scintillation levels. The correlation coefficient between scintillation indices and phase residual standard deviation could be as high as 0.8262 and 0.8442 for S_4 and σ_ϕ , respectively. As only two days of data were analysed, there was no attempt to develop statistical models to describe the relationship between scintillation levels and the standard deviation of phase residuals. This will be the focus of follow on study.
4. Compared with satellite elevation, scintillation levels showed a stronger influence on the phase residuals. Under the same scintillation level, the phase residual fluctuations varied slightly for all the elevations. However, both amplitude and phase scintillation were seen to greatly increase the standard deviation of phase residuals. Under weak scintillation conditions, the standard deviations were below 0.005 m. However, the standard deviation of carrier phase residuals increased to 0.03 m in the presence of extremely strong scintillation.

These results are of great importance in better understanding low latitude scintillation effects on PPP. This study could also contribute to the modelling of ionospheric scintillation effects on carrier phase residuals and to the development of scintillation mitigation tools for satellite-based positioning algorithms.

ACKNOWLEDGMENTS

The authors wish to thank the TREASURE project (www.treasure-gnss.eu), funded by the European Union's Horizon 2020 Research and Innovation Programme under the Marie Skłodowska-Curie Actions grant agreement No. 722023. The GNSS scintillation data were collected from the Hok Tsui station, Hong Kong, which was jointly installed by Dr. Jade Morton's group at the University of Colorado, USA and Dr. George Zhizhao Liu's group at the Hong Kong Polytechnic University, Hong Kong. The GNSS scintillation receiver was provided by Dr. Jade Morton's group at the University of Colorado, USA. Authors also want to thanks to Xiangdong An from Wuhan University and Brian Weaver from Nottingham Geospatial Institute for the helpful discussion.

REFERENCES

1. Kintner, P. M., Kil, H., Beach, T. L. and de Paula, E. R., "Fading Timescales Associated with GPS Signals and Potential Consequences," *Radio Science*, Vol. 36, No. 4, 2001, pp. 731-743.
2. Basu, S., MacKenzie, E. and Basu, S., "Ionospheric Constraints on VHF/UHF Communications Links during Solar Maximum and Minimum Periods," *Radio Science*, Vol. 23, No. 03, 1988, pp. 363-378.
3. Conker, R. S., El-Arini, M. B., Hegarty, C. J. and Hsiao, T., "Modeling the Effects of Ionospheric Scintillation on GPS/satellite-based Augmentation System Availability," *Radio Science*, Vol. 38, No. 1, 2003, pp. 1-1-1-23.
4. Knight, M. and Finn, A., "The Effects of Ionospheric Scintillations on GPS," *Proceedings of the 11th International Technical Meeting of the Satellite Division of The Institute of Navigation (ION GPS 1998)*, Nashville, TN, September 1998, pp. 673-685.
5. Sreeja, V., Aquino M. and Elmas Z. G., "Impact of ionospheric scintillation on GNSS receiver tracking performance over Latin America: Introducing the concept of tracking jitter variance maps," *Space Weather*, Vol. 9, No. 10, 2011, pp. 1-6.
6. Humphreys, T. E., Psiaki, M. L. and Kintner, P. M., "GPS Carrier Tracking Loop Performance in the presence of Ionospheric Scintillations," *Proceedings of the 18th International Technical Meeting of the Satellite Division of The Institute of Navigation (ION GNSS 2005)*, Long Beach, CA, September 2005, pp. 156-167.

7. Pi, X., Iijima, B. A. and Lu, W., "Effects of Ionospheric Scintillation on GNSS-Based Positioning," *Navigation*, Vol. 64, No. 1, 2017, pp. 3-22.
8. Linty, N., Minetto, A., Dovis, F. and Spogli, L., "Effects of phase scintillation on the GNSS positioning error during the September 2017 storm at Svalbard," *Space Weather*, Vol. 16, No. 9, 2018, pp. 1317-1329.
9. Park, J., Veetil, S. V., Aquino, M., Yang, L. and Cesaroni, C., "Mitigation of ionospheric effects on GNSS positioning at low latitudes," *Navigation*, Vol. 64, No. 1, 2017, pp. 67-74.
10. Luo, X., Lou, Y., Xiao, Q., Gu, S., Chen, B. and Liu, Z., "Investigation of ionospheric scintillation effects on BDS precise point positioning at low-latitude regions," *GPS Solutions*, Vol. 22, No. 3, 2018, pp. 63.
11. Van Dierendonck, A. J., Klobuchar, J. and Hua, Q., "Ionospheric Scintillation Monitoring Using Commercial Single Frequency C/A Code Receivers," *Proceedings of the 6th International Technical Meeting of the Satellite Division of The Institute of Navigation (ION GPS 1993)*, Salt Lake City, UT, September 1993, pp. 1333-1342.
12. Van Dierendonck, A. J. and Arbesser-Rastburg, B., "Measuring Ionospheric Scintillation in the Equatorial Region Over Africa, Including Measurements From SBAS Geostationary Satellite Signals," *Proceedings of the 17th International Technical Meeting of the Satellite Division of The Institute of Navigation (ION GNSS 2004)*, Long Beach, CA, September 2004, pp. 316-324.
13. Van Dierendonck, A. J., "Eye on the Ionosphere: Measuring Ionospheric Scintillation Effects from GPS Signals," *GPS Solutions*, Vol. 2, No. 4, 1999, pp. 60-63.
14. Strangeways, H. J., Ho, Y. H., Aquino, M. H., Elmas, Z. G., Marques, H. A., Monico, J. F. and Silva, H. A., "On determining spectral parameters, tracking jitter, and GPS positioning improvement by scintillation mitigation," *Radio Science*, Vol. 46, No. 6, 2011.
15. Marques, H. A. S., Monico, J. F. G. and Marques, H. A., "Performance of the L2C civil GPS signal under various ionospheric scintillation effects," *GPS Solutions*, Vol. 20, No. 2, 2016, pp. 139-149.
16. Hegarty, C., El-Arini, M. B., Kim, T. and Ericson, S., "Scintillation modeling for GPS-wide area augmentation system receivers," *Radio Science*, Vol. 36, No. 5, 2001, pp. 1221-1231.
17. Liu, Z., Xu, R., Morton, J., Xu, J., Pelgrum, W., Taylor, S., Chen, W. and Ding, X., "A Comparison of GNSS-based Ionospheric Scintillation Observations in North and South Hong Kong," *Proceedings of the ION 2013 Pacific PNT Meeting, Honolulu, Hawaii, April 2013*, pp. 694-705.